Comparison of two gravity recovery algorithms based on the variational equation approach

Muhammad Athar Javaid
Institute for Geodesy
uni-Stuttgart, Germany
Email: javaid@gis.uni-stuttgart

Wolfgang Keller
Institute for Geodesy
uni-Stuttgart, Germany
Email: wolfgang.keller@gis.uni-stuttgart.de

Abstract*—Gravity field recovery using space technology has evolved during the last two decades. Several dedicated satellite missions have been sent to the space to get more accurate and up-to-date gravity field information, including, Challenging Minisatellite Payload (CHAMP), Gravity Recovery and Climate Experiment (GRACE) and Gravity field and Ocean Circulation Explorer (GOCE), launched on 15 July 2000, 17 March 2002 and 17 March 2009, respectively. GRACE is the extended version of the CHAMP. The major difference is that the CHAMP is an example of high-low satellite-to-satellite tracking (HL-SST) while the GRACE is an example of low-low satellite-to-satellite tracking (LL-SST) system. We observe the inter-satellite range rates of GRACE tandem constellation. The variation in inter-satellite range is due to the gravity field variation underneath the satellites. There are several methods in practice to recover the gravity field from range rate observation such as *acceleration approach, short arc approach and energy balance approach*. The most accurate and widely used is the *variational equation approach*, however numerically costly (Keller, 2014). This paper states the variational equation method in detail and compare the performance of the its two different implementation methods i.e. *analytical* and *variation of constant* method. The study shows that the computation time for the *variation of constant* method has reduced tremendously while achieving the same level of accuracy.

I. Introduction

GRACE is a pair of free falling gravity recovery satellites. It is launched by National Aeronautics and Space Administration (NASA), USA and the German Space Agency (DLR) under the NASA Earth System Science Pathfinder Program . According to the details, regions of slightly stronger gravity affect the leading satellite first, accelerating it slightly stronger than the trailing satellite, (NASA, 2002). The satellite constellation of two low earth orbiting satellites in which we measure the inter satellite range rates is called as low-low satellite-to-satellite tracking (LL-SST). (Rummel et al., 2002)

The gravitational potential V at any location (r, θ, λ) on Earth is represented in terms of SH coefficients, as given in (1), for details, see (Heiskanen and Moritz, 1967). Gravity field recovery in the form of spherical harmonic SH coefficients from range rates measurements can be considered as a differential orbit improvement process.

$$\begin{aligned} V(r,\theta,\lambda) &= \frac{GM}{R}\sum_{\ell=0}^{\infty}\left(\frac{R}{r}\right)^{\ell+1}\sum_{m=0}^{\ell}P_{\ell m}(\cos\theta) \\ &\quad \left[C_{\ell m}\cos(m\lambda)+S_{\ell m}\sin(m\lambda)\right]. \end{aligned} \tag{1}$$

We use orbit integration, firstly, to generate the position and velocity vectors of the two satellites and later to compute the partial derivative of the position and velocity vectors with respect to the a priori SH coefficients. Section II states the mathematical details of the orbit integration, computation of the position and velocity vectors of the two satellites and coordinates conversion. In section III we explain the process of taking the partial derivatives of the position and velocity vectors with respect to the a priori SH coefficients. In section IV, we introduce *variation of constant* method as an alternate method to compute the partials of position and velocity vectors. In section V we state the process of coefficient estimation and compare the performance of the variation of constant method with the analytical method. Results and noise analyses are presented in section VI.

In subsection I-A we show how to arrange and visualize the SH coefficients and in subsection I-B we compute the range rates from the position vectors of the two satellites.

In this study we simulate the GRACE system with certain simplifications. We ignore all kinds of tides during the orbit integration. Furthermore, we consider only the Greenwich Apparent Sidereal Time (GAST) to convert the coordinates of position and velocity vectors from Earth fixed system to the inertial system.

A. Spherical harmonic (SH) coefficients

The simulation process recovers the SH coefficients, up to maximum degree and order $\ell_{max} = 90$. They are usually arranged in a special matrix format called SC format, in which sine ($S_{\ell,m}$) and cosine ($C_{\ell,m}$) coefficients, with degree ℓ and order m, are placed in triangular format, as illustrated in the following matrix.

$$\begin{pmatrix} & & & C_{0,0} & & & \\ & & S_{1,1} & C_{1,0} & C_{1,1} & & \\ & S_{2,1} & S_{2,1} & C_{2,0} & C_{2,1} & C_{2,2} & \\ \iddots & & \vdots & \vdots & \vdots & & \ddots \\ S_{\ell,m} & \ldots & S_{\ell,1} & C_{\ell,0} & C_{\ell,1} & \ldots & C_{\ell,m} \end{pmatrix}$$

We use the SC format to visualize the SH coefficients. We take their absolute values and plot them in logarithmic scale, as presented in Fig. 1. For this paper, we utilize the SC format to present the recovered SH coefficients and their empirical and formal errors. Later in this document, we denote the SH coefficients as $p_{\mathbb{L}}$, where $\mathbb{L} = 1, ..., L$ and $L = (\ell_{max} + 1)^2$ is total number of SH coefficients up to ℓ_{max}.

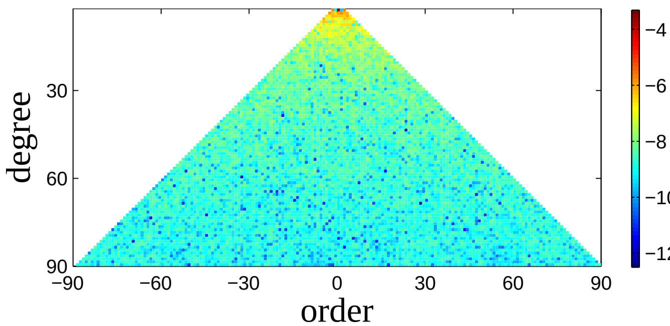

Fig. 1: A colored representation of absolute values of SH coefficients on logarithmic scale starting form degree 2.

B. ll-SST Observables

Inter-satellite range rates are the key observations form the GRACE system. Since orbit integration process produces the position and velocity vectors. Therefore, here we state the method to derive the range rates from the position and velocity vectors.

Let the position $\mathbf{x}$, velocity $\dot{\mathbf{x}}$ and acceleration $\ddot{\mathbf{x}}$ vectors of GRACE satellites are represented as,

$$\mathbf{x}_s = \{x_s, y_s, z_s\}, \quad \dot{\mathbf{x}}_s = \{\dot{x}_s, \dot{y}_s, \dot{z}_s\}, \quad \ddot{\mathbf{x}}_s = \{\ddot{x}_s, \ddot{y}_s, \ddot{z}_s\}, \tag{2}$$

where s = A,B, represents the two satellites i.e. A is the leading and B is the trailing. The difference between the position, velocity and acceleration vectors are,

$$\delta\mathbf{x} = \mathbf{x}_{\mathrm{B}} - \mathbf{x}_{\mathrm{A}}, \quad \delta\dot{\mathbf{x}} = \dot{\mathbf{x}}_{\mathrm{B}} - \dot{\mathbf{x}}_{\mathrm{A}}, \quad \delta\ddot{\mathbf{x}} = \ddot{\mathbf{x}}_{\mathrm{B}} - \ddot{\mathbf{x}}_{\mathrm{A}} \tag{3}$$

and we can get the scalar inter-satellite range as

$$\rho = \sqrt{\langle\delta\mathbf{x}|\delta\mathbf{x}\rangle} = |\delta\mathbf{x}|, \tag{4}$$

while the unit vector in the direction of the inter-satellite range is

$$\mathbf{e} = [e_x \; e_y \; e_z]^\top = \frac{\delta\mathbf{x}}{\rho}. \tag{5}$$

The inter-satellite range vector can be written as,

$$\delta\mathbf{x} = \rho\mathbf{e}. \tag{6}$$

Differentiating (6) results in range rate:

$$\delta\dot{\mathbf{x}} = \dot{\rho}\mathbf{e} \; + \; \rho\dot{\mathbf{e}}, \tag{7}$$

$\mathbf{e}$ is a unit vector and therefore

$$\mathbf{e}\cdot\mathbf{e} = 1 \;\Rightarrow\; \mathbf{e}\cdot\dot{\mathbf{e}} = 0. \tag{8}$$

Hence, the time derivative $\dot{\mathbf{e}}$ of the line of sight vector (LOS) is perpendicular to the LOS vector itself. The vector $\dot{\mathbf{e}}$ itself is not a unit vector. Therefore (7) becomes

$$\delta\dot{\mathbf{x}}\cdot\mathbf{e} = \dot{\rho}\cdot\mathbf{e}\cdot\mathbf{e} + \rho\cdot\dot{\mathbf{e}}\cdot\mathbf{e} \tag{9}$$

or

$$\dot{\rho} = \delta\dot{\mathbf{x}}\cdot\mathbf{e}. \tag{10}$$

II. Orbit Integration

The motion of a satellite around a celestial body can be expressed as second order differential equation. In this section, *firstly*, we consider that the Earth is a body of homogeneous mass and therefore exerts a constant force, which does not represents the reality, therefore, *secondly*, we present the case considering Earth as non-homogeneous.

From the *law of gravitation* we know that force of gravitation $\mathbf{F}$ between satellite and the Earth is given by $\mathbf{F} = G\frac{Mm}{r^2}\boldsymbol{e}_r$, with the gravitational constant G, the mass of the Earth M, the mass of the satellite m, the distance between the satellite and the center of the Earth r and the direction vector along the force of gravitation $\boldsymbol{e}_r$. Furthermore, from *Newton's second law of motion* we know that $\mathbf{F} = m\mathbf{a}$ or $m\ddot{\mathbf{x}}$, therefore, the equation of motion of a satellite around the Earth under the influence of a homogeneous central force can be written as

$$m\ddot{\mathbf{x}} = -G\frac{Mm}{r^2}\boldsymbol{e}_r. \tag{11}$$

We know that *vector* = *magnitude* × *direction* therefore $\mathbf{x} = |r|\cdot\boldsymbol{e}_r$ or $\boldsymbol{e}_r = \frac{\mathbf{x}}{|r|}$. The (11) becomes,

$$m\ddot{\mathbf{x}} = -\frac{GM}{r^3}m\mathbf{x}, \tag{12}$$

and finally the second order differential equation is given as,

$$\ddot{\mathbf{x}} + \frac{GM}{r^3}\mathbf{x} = 0. \tag{13}$$

Whereas for the case of a non-homogeneous central force, the equation becomes,

$$\ddot{\mathbf{x}} + \frac{GM}{r^3}\mathbf{x} = f(\mathbf{x}). \tag{14}$$

Now consider the substitutions, $u = \mathbf{x}$, then,

$$\begin{aligned} u' &= \dot{\mathbf{x}} = v \\ v' &= \ddot{\mathbf{x}} = -\tfrac{GM}{r(u)^3}u + f(u). \end{aligned} \tag{15}$$

Written in matrix format

$$\begin{bmatrix} u' \\ v' \end{bmatrix} = \begin{bmatrix} 0 & 1 \\ -\frac{GM}{r(u)^3} & 0 \end{bmatrix} \begin{bmatrix} u \\ v \end{bmatrix} + \begin{bmatrix} 0 \\ f(u) \end{bmatrix}, \tag{16}$$

where $f(u)$ represents the non homogeneous part of the gravity. Note that from the beginning of this section we are working in the inertial frame where the vectors are presented with Cartesian coordinates. This means that the position vectors of the satellites are actually the distance of the satellite in meters from center of the Earth in $\{x, y, z\}$ directions. The issue is that the non-homogeneous part of the (16) is originally a function dependent upon geographic locations of the Earth, therefore, it is required to transform its partial derivatives in the inertial frame. Note that the notations l, e and i present local, earth fixed and inertial coordinate systems, respectively. (17) represents the original function.

$$f(u) = T = \frac{GM}{R}\sum_{\ell=2}^{L}\left(\frac{R}{r}\right)^{\ell+1}\sum_{m=0}^{\ell}P_{\ell m}(\cos\theta) \quad [\nabla C_{\ell m}\cos(m\lambda) + \nabla S_{\ell m}\sin(m\lambda)]. \tag{17}$$

For this simulation, T is differentiated w.r.t spherical coordinates r, θ, λ, and denoted as gradients g_x, g_y, g_z, in a local north oriented frame. We define the local north oriented frame as,

- 1st axis, x is oriented in radial direction
- 2nd axis, y points the North pole/rotation axis
- 3rd axis, z points tangential in lambda direction

and the gradients are,

$$\begin{aligned}
g_x^l = \quad & \frac{\partial T}{\partial r} = & -\frac{GM}{r^2}\sum_{\ell=2}^{L}\left(\frac{R}{r}\right)^{\ell}\sum_{m=0}^{\ell}P_{\ell m}(\cos\theta) \\
&& [\nabla C_{\ell m}\cos(m\lambda) + \nabla S_{\ell m}\sin(m\lambda)] \\
&& (\ell+1), \\
g_y^l = \quad \frac{1}{r} & \frac{\partial T}{\partial \theta} = & -\frac{GM}{r^2}\sum_{\ell=2}^{L}\left(\frac{R}{r}\right)^{\ell}\sum_{m=0}^{\ell}P'_{\ell m}(\cos\theta) \\
&& [\nabla C_{\ell m}\cos(m\lambda) + \nabla S_{\ell m}\sin(m\lambda)] \\
&& \sin\theta, \\
g_z^l = \quad \frac{1}{r\sin\theta} & \frac{\partial T}{\partial \lambda} = & \frac{GM}{r^2}\sum_{\ell=2}^{L}\left(\frac{R}{r}\right)^{\ell}\sum_{m=0}^{\ell}P_{\ell m}(\cos\theta) \\
&& [\nabla - C_{\ell m}\sin(m\lambda) + \nabla S_{\ell m}\cos(m\lambda)] \\
&& m\frac{1}{\sin\theta}.
\end{aligned} \tag{18}$$

The superscript l on g_x^l, g_y^l, g_z^l shows that the gradients are in the local north oriented coordinate system. We can write it in vector format as: $[g_x, g_y, g_z]_l^\top$. To convert it into the Earth-fixed frame we need the following transformation matrix.

$$\mathbf{R}_l^{\mathrm{e}} = \begin{bmatrix} \sin\theta\cos\lambda & -\cos\theta\cos\lambda & -\sin\lambda \\ \sin\theta\sin\lambda & -\cos\theta\sin\lambda & \cos\lambda \\ \cos\theta & \sin\theta & 0 \end{bmatrix}, \tag{19}$$

where $\mathbf{R}_l^{\mathrm{e}}$ means the rotation matrix form local to earth fixed system. Furthermore, from Earth-fixed frame to inertial frame we need to rotate the vectors through $\mathbf{R}_e^i = \mathbf{R}_3(-\mathrm{GAST})$ rotation matrix. Eventually, the complete transformation turns out to be $\mathbf{R}_l^i = \mathbf{R}_e^i\mathbf{R}_l^e$, and we can show the complete coordinate transformation as,

$$\begin{bmatrix} g_x \\ g_y \\ g_z \end{bmatrix}_i = \mathbf{R}_l^i \begin{bmatrix} g_x \\ g_y \\ g_z \end{bmatrix}_l. \tag{20}$$

Now if we write the (16) in its components' form and insert the partial derivatives of $f(u)$ from (20), we will get the following formulation,

$$\begin{bmatrix} u_x' \\ u_y' \\ u_z' \\ v_x' \\ v_y' \\ v_z' \end{bmatrix} = \left[\begin{array}{c|c} \mathbf{0}_{3\times3} & \mathbf{I}_{3\times3} \\ \hline \mathbf{I}_{3\times3}\cdot -\frac{GM}{r(u)^3} & \mathbf{0}_{3\times3} \end{array}\right] \begin{bmatrix} u_x \\ u_y \\ u_z \\ v_x \\ v_y \\ v_z \end{bmatrix} + \begin{bmatrix} 0 \\ 0 \\ 0 \\ g_x \\ g_y \\ g_z \end{bmatrix}, \tag{21}$$

here $\mathbf{0}_{3\times3}$ is a null matrix and $\mathbf{I}_{3\times3}$ identity matrix, where index i from gradients has been dropped, since all quantities are in the inertial system.

III. Partial derivatives of position and velocity with respect to unknown $p_{\mathbb{L}}$

Gravity field recovery from range rates measurements can be considered as a differential orbit improvement process. True range rates measurements can be expressed as truncated Taylor series with respect to the unknown $p_{\mathbb{L}}$ about the a priori range rates. Before moving forward to state formally the observation equation for the ll-SST, let us first derive the partial derivatives of the position and the velocity w.r.t. $p_{\mathbb{L}}$. To start, let us take

$$\ddot{\mathbf{x}} = \nabla U + \nabla T \tag{22}$$

where $\boldsymbol{U}$ represents the homogeneous part of the gravitational force and equals to $\frac{GM}{r^3}\mathbf{x}$ and T represents the non-homogeneous part of the gravitational force and given in (17). Differentiating it with respect to $p_{\mathbb{L}}$, we will get

$$\frac{\partial\ddot{\mathbf{x}}}{\partial p_{\mathbb{L}}} = \frac{\partial(\nabla U)}{\partial p_{\mathbb{L}}} + \frac{\partial(\nabla T)}{\partial p_{\mathbb{L}}}. \tag{23}$$

Apply the chain rule on the first term of right hand side

$$\frac{\partial\ddot{\mathbf{x}}}{\partial p_{\mathbb{L}}} = \frac{\partial(\nabla U)}{\partial \mathbf{x}}\frac{\partial\mathbf{x}}{\partial p_{\mathbb{L}}} + \frac{\partial(\nabla T)}{\partial p_{\mathbb{L}}}, \tag{24}$$

consider the definition

$$\boldsymbol{\xi} = \frac{\partial\mathbf{x}}{\partial p_{\mathbb{L}}} \tag{25}$$

and (24) becomes

$$\ddot{\boldsymbol{\xi}} = \nabla^2 U\boldsymbol{\xi} + \frac{\partial(\nabla T)}{\partial p_{\mathbb{L}}}. \tag{26}$$

Similar to the case of orbit integration we can write the (26) into two first order differential equations. The system of equation in matrix format becomes,

$$\begin{bmatrix} \xi_x' \\ \xi_y' \\ \xi_z' \\ \dot{\xi}_x' \\ \dot{\xi}_y' \\ \dot{\xi}_z' \end{bmatrix} = \left[\begin{array}{c|c} \mathbf{0}_{3\times3} & \mathbf{I}_{3\times3} \\ \hline \mathbf{a}_{3\times3} & \mathbf{0}_{3\times3} \end{array}\right] \begin{bmatrix} \xi_x \\ \xi_y \\ \xi_z \\ \dot{\xi}_x \\ \dot{\xi}_y \\ \dot{\xi}_z \end{bmatrix} + \begin{bmatrix} 0 \\ 0 \\ 0 \\ \frac{\partial(g_x)}{\partial p_{\mathbb{L}}} \\ \frac{\partial(g_y)}{\partial p_{\mathbb{L}}} \\ \frac{\partial(g_z)}{\partial p_{\mathbb{L}}} \end{bmatrix}, \tag{27}$$

$$\text{and} \quad \mathbf{a}_{3\times 3} = \mathbf{R}_l^i \nabla^2 U \mathbf{R}_i^l,$$

$$\text{where} \quad \nabla^2 U = \begin{bmatrix} U_{xx} & U_{xy} & U_{xz} \\ U_{yx} & U_{yy} & U_{yz} \\ U_{zx} & U_{zy} & U_{zz} \end{bmatrix}.$$

The components of the matrix $\nabla^2 U$ are

$$\begin{aligned}
U_{xx} =& \tfrac{\partial}{\partial r}(\tfrac{\partial V}{\partial r}), \\
U_{yy} =& \tfrac{1}{r}\tfrac{\partial}{\partial \theta}(\tfrac{1}{r}\tfrac{\partial V}{\partial \theta}) + \tfrac{1}{r}\tfrac{\partial V}{\partial r}, \\
U_{zz} =& \tfrac{1}{r\sin\theta}\tfrac{\partial}{\partial \lambda}(\tfrac{1}{r\sin\theta}\tfrac{\partial V}{\partial \lambda}) + \tfrac{1}{r}\tfrac{\partial V}{\partial r} - \tfrac{1}{r^2\tan\theta}\tfrac{\partial V}{\partial \theta}, \\
U_{xy} =& \tfrac{\partial}{\partial r}(\tfrac{1}{r}\tfrac{\partial V}{\partial \theta}) - \tfrac{1}{r^2}\tfrac{\partial V}{\partial \theta}, \\
U_{xz} =& \tfrac{1}{r\sin\theta}\tfrac{\partial}{\partial \lambda}(\tfrac{\partial V}{\partial r}) - \tfrac{1}{r\sin\theta}\tfrac{\partial V}{\partial \lambda}, \\
U_{yz} =& \tfrac{1}{r\sin\theta}\tfrac{\partial}{\partial \lambda}(\tfrac{1}{r}\tfrac{\partial V}{\partial \theta}),
\end{aligned}$$

where $U_{xy} = U_{yx}, U_{xz} = U_{zx}$ and $U_{yz} = U_{zy}$ see, (Wermuth, 2008). While solving the components for the homogeneous part we get

$$\nabla^2 U = \begin{bmatrix} 2\frac{GM}{r^3} & 0 & 0 \\ 0 & -\frac{GM}{r^3} & 0 \\ 0 & 0 & -\frac{GM}{r^3} \end{bmatrix}.$$

TABLE I: Initial osculating Kepler elements of the two GRACE satellites for simulation

Element/Sat.	Sat. A	Sat. B
a in [m]	6838136.6	6838136.6
e	0.002	0.002
i in [°]	89	89
ω in [°]	0	0
Ω in [°]	0	0
ν in [°]	+1	−1

IV. Simulation

This section states the sequential processing of the variational equation approach. We start the process with the a priori orbit integration. First of all, the initial state vector is created and filled with the osculating Kepler elements (KE). The values are given in the Table I. For integration, the KE are converted to the Cartesian coordinates of the position and velocity vectors, see (Seeber, 2003). Now, the a priori orbits $u_{o\mathrm{A}}(t)$ and $v_{o\mathrm{B}}(t)$ are integrated for (t) epochs for GRACE satellites A and B, respectively, using EGM96 an a priori field and therefore a priori inter-satellite range rates $\dot{\rho}_0(t)$ are computed. Since we are not using the True inter-satellite range rates from GRACE, therefore we also generate them using the orbit integration. Therefore, $u_\mathrm{A}(t)$, $v_\mathrm{B}(t)$ and $\dot{\rho}(t)$ are computed using GGM08 as true fields. The process is also expressed as flow chart in Fig. 2. Since K-band measurements are not used, therefore, $\dot{\rho}(t)$ will serve the purpose of true range rates. Whereas, the difference of the two range rates i.e $\delta\dot{\rho}(t) = \dot{\rho}(t) - \dot{\rho}_0(t)$ will act as the observation y of the our least square adjustment process, discussed in the section V. This leave us with the task of generating the partial derivatives. To accomplish this task, two methods, i.e. analytical and Gaussian quadrature method, are presented here, for details, see, (Beutler, 2005). In the following two subsections the implementation of the both methods is described in detail.

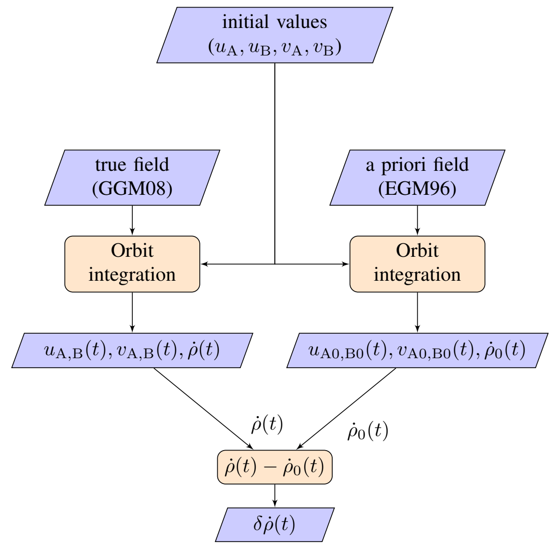

Fig. 2: Flow chart for computing range rates.

A. *Analytical method*

One way of dealing with the issue of generating the partial is to consider the SH coefficients separately from each other and generating partials sequentially. Before going into the details, please consider that the initial value of the partials i.e. $\boldsymbol{\xi} = 0$, $\dot{\boldsymbol{\xi}} = 0$. The homogeneous and non-homogeneous parts of (27) are solved together iteratively. During one iteration we can get the partials with respect to only one coefficient. Consequently, we have to iterate the whole process as many times as coefficients we have to recover. To elaborate this let us consider highest degree and order $\ell_{max} = 20$, therefore total number of coefficients L = 441, we can ignore the first four coefficients, i.e. C_{00}, C_{10}, C_{11} and S_{10}, which leaves us with 437 coefficients. This means that the procedure of generating partial will be repeated 437 times and consume a lot of time even if we simulate it for only one-day arc i.e. $t = 0, 10, 20, ..., 86400$. The advantage of this procedure is that we can process a single selected coefficients as well.

B. *Gaussian quadrature method*

A lot of computation time and resources are required to generate the partial derivatives one by one, therefore, the *variation of constants* or *variation of parameters* method is used. The salient feature of the process is that the homogeneous and non-homogeneous parts of (27) are solved separately. First of all, by using the satellites positions $u_0(t)$, the non-homogeneous part of (27) is solved i.e. we get the individual numerical values for the $g_x(t)$ $g_y(t)$ and $g_z(t)$ with respect to all SH coefficients.

Now using an a priori field the satellite $u_0(t), v_0(t)$, the homogeneous part of the (27) is integrated. The process is iterated six times and each time, different initial values for

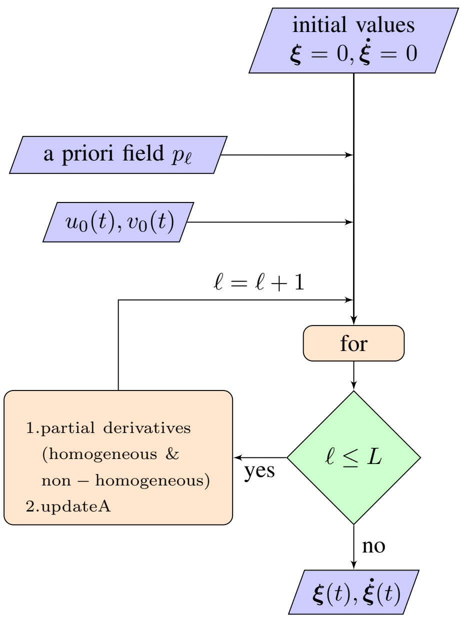

Fig. 3: Flow chart for analytical method.

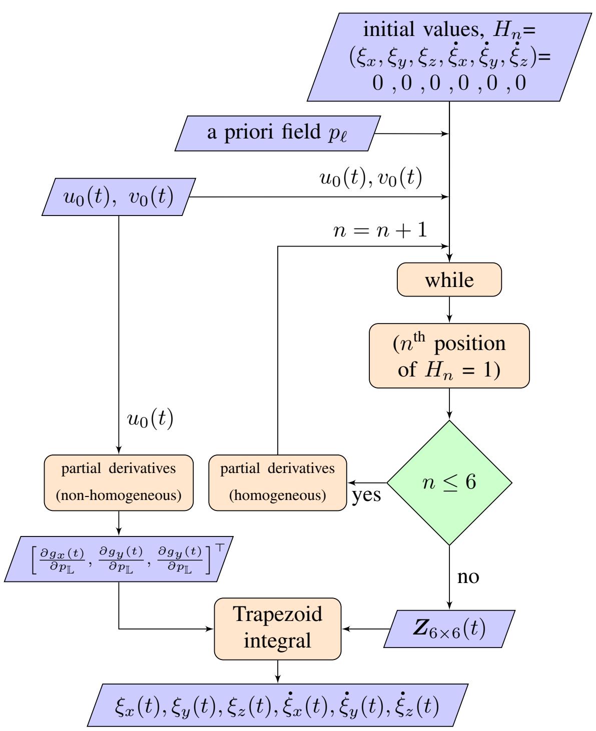

Fig. 4: Flow chart for Gaussian quadrature method.

the partials are used. For instance, $\zeta_i(t)$ is the set of initial values where $i = 1, 2, ..., 6$ (no. of iterations), then, for each iteration, the set of initial values for the first epoch are given as

$$\begin{array}{c} \begin{array}{cccccc} \zeta_1 & \zeta_2 & \zeta_3 & \zeta_4 & \zeta_5 & \zeta_6 \end{array} \\ \left[\begin{array}{c|c|c|c|c|c} 1 & 0 & 0 & 0 & 0 & 0 \\ 0 & 1 & 0 & 0 & 0 & 0 \\ 0 & 0 & 1 & 0 & 0 & 0 \\ 0 & 0 & 0 & 1 & 0 & 0 \\ 0 & 0 & 0 & 0 & 1 & 0 \\ 0 & 0 & 0 & 0 & 0 & 1 \end{array}\right] \end{array} = \boldsymbol{Z}(t = 0) \ . \tag{28}$$

Let $[0\ 0\ 0\ \frac{\partial g_x(t)}{\partial p_{\mathbb{L}}}, \frac{\partial g_y(t)}{\partial p_{\mathbb{L}}}, \frac{\partial g_y(t)}{\partial p_{\mathbb{L}}}]^\top = Y(t)$, and $\dot{\alpha}_r(t)$ with $r = 1, ..., 6$ are six unknowns. We can write,

$$\boldsymbol{Z}_{6\times6}(t)\ \dot{\alpha}_{6\times1}(t) = Y_{6\times1}(t) \ , \tag{29}$$

or

$$\dot{\alpha}(t) = \boldsymbol{Z}^{-1}(t) Y(t) \ . \tag{30}$$

After solving the above equation, $\dot{\alpha}_{6\times1}(t)$ is converted into $\alpha_{6\times1}(t)$ using the trapezoid integral. To get the cumulative value at every epoch t, the cumulative trapezoid function is used. Finally, the two solutions, i.e. the homogeneous from (28) and the particular from cumulative trapezoid integral, are solved together for each epoch t in the following way

$$\sum_{q=1}^{6} \zeta_q(t) \alpha_q(t) = \begin{bmatrix} \xi_x(t) \\ \xi_y(t) \\ \xi_z(t) \\ \dot{\xi}_x(t) \\ \dot{\xi}_y(t) \\ \dot{\xi}_z(t) \end{bmatrix} . \tag{31}$$

An alternative to the trapezoid integral is the Simpson integral. The simulation proved that the empirical and formal error of the two methods are same, however the trapezoid integral is faster then the Simpson integral. The results of simulation using Simpson integral are not shown here.

V. Coefficient Estimation

As stated in the last section that the gravity field recovery from range rates measurements can be considered as a differential orbit improvement process, therefore, $\dot{\rho}(t)$ is expressed as truncated Taylor series with respect to $p_{\mathbb{L}}$ about $\dot{\rho}_0(t)$. (Jäggi et al., 2010). Let us formally express it as,

$$\dot{\rho}(t) = \dot{\rho}_0(t) + \left[\frac{\partial \dot{\rho}_0}{\partial p_1}(t), ..., \frac{\partial \dot{\rho}_0}{\partial p_L}(t)\right] \begin{bmatrix} \Delta p_1 \\ \vdots \\ \Delta p_L \end{bmatrix} , \tag{32}$$

so the final observation equation becomes,

$$\delta\dot{\rho}(t) = \left[\frac{\partial\dot{\rho}_0}{\partial p_1}(t), ..., \frac{\partial\dot{\rho}_0}{\partial p_L}(t)\right] \begin{bmatrix} \Delta p_1 \\ \vdots \\ \Delta p_L \end{bmatrix}, \qquad (33)$$

where $\delta\dot{\rho}(t) = \dot{\rho}(t) - \dot{\rho}_0(t)$. For simplicity, let us drop (t) and the index 0, for each $p_{\mathbb{L}}$ we write

$$\frac{d\dot{\rho}}{dp_{\mathbb{L}}} = \frac{\partial\dot{\rho}}{\partial\mathbf{x}_{\mathrm{A}}}\frac{\partial\mathbf{x}_{\mathrm{A}}}{\partial p_{\mathbb{L}}} + \frac{\partial\dot{\rho}}{\partial\dot{\mathbf{x}}_{\mathrm{A}}}\frac{\partial\dot{\mathbf{x}}_{\mathrm{A}}}{\partial p_{\mathbb{L}}} + \frac{\partial\dot{\rho}}{\partial\mathbf{x}_{\mathrm{B}}}\frac{\partial\mathbf{x}_{\mathrm{B}}}{\partial p_{\mathbb{L}}} + \frac{\partial\dot{\rho}}{\partial\dot{\mathbf{x}}_{\mathrm{B}}}\frac{\partial\dot{\mathbf{x}}_{\mathrm{B}}}{\partial p_{\mathbb{L}}}, \qquad (34)$$

or after using (25)

$$\frac{d\dot{\rho}}{dp_{\mathbb{L}}} = \frac{\partial\dot{\rho}}{\partial\mathbf{x}_{\mathrm{A}}}\boldsymbol{\xi}_{\mathrm{A}} + \frac{\partial\dot{\rho}}{\partial\dot{\mathbf{x}}_{\mathrm{A}}}\dot{\boldsymbol{\xi}}_{\mathrm{A}} + \frac{\partial\dot{\rho}}{\partial\mathbf{x}_{\mathrm{B}}}\boldsymbol{\xi}_{\mathrm{B}} + \frac{\partial\dot{\rho}}{\partial\dot{\mathbf{x}}_{\mathrm{B}}}\dot{\boldsymbol{\xi}}_{\mathrm{B}}, \qquad (35)$$

Now after inserting the value of $\dot{\rho}$ form 10 we can write,

$$\frac{d\dot{\rho}}{dp_{\mathbb{L}}} = \frac{\partial(\delta\dot{\mathbf{x}}\mathbf{e})}{\partial\mathbf{x}_{\mathrm{A}}}\boldsymbol{\xi}_{\mathrm{A}} + \frac{\partial(\delta\dot{\mathbf{x}}\mathbf{e})}{\partial\dot{\mathbf{x}}_{\mathrm{A}}}\dot{\boldsymbol{\xi}}_{\mathrm{A}} + \frac{\partial(\delta\dot{\mathbf{x}}\mathbf{e})}{\partial\mathbf{x}_{\mathrm{B}}}\boldsymbol{\xi}_{\mathrm{B}} + \frac{\partial(\delta\dot{\mathbf{x}}\mathbf{e})}{\partial\dot{\mathbf{x}}_{\mathrm{B}}}\dot{\boldsymbol{\xi}}_{\mathrm{B}}, \qquad (36)$$

after derivation, we can write,

$$\frac{d\dot{\rho}}{dp_{\mathbb{L}}} = -\frac{1}{\rho}\left(\delta\dot{\mathbf{x}} - \mathbf{e}\dot{\rho}\right)^{\top}\boldsymbol{\xi}_{\mathrm{A}} - \mathbf{e}\dot{\boldsymbol{\xi}}_{\mathrm{A}} + \frac{1}{\rho}\left(\delta\dot{\mathbf{x}} - \mathbf{e}\dot{\rho}\right)^{\top}\boldsymbol{\xi}_{\mathrm{B}} + \mathbf{e}\dot{\boldsymbol{\xi}}_{\mathrm{B}}, \qquad (37)$$

Note that the quantities for satellite A and satellite B are same but with opposite signs. Solving (37) for each $p_{\mathbb{L}}$ leads us to the formulation of the design matrix A. While the observation y has already been computed in section IV. Now Least-Squares adjustment is used to get the improved SH coefficients. Whereas, by adding them to the a priori SH coefficients, we will get the estimated SH coefficients.

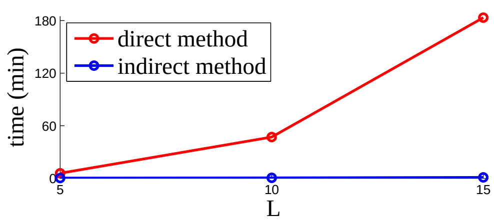

Fig. 5: Time consumption comparison of the two method

VI. Results

Here, we analyze the time consumption and the accuracy of the recovered SH coefficients of the two methods. The goal was to recover the coefficients under the same conditions, therefore, no random noise has been added to the observation. Fig.5 shows that the analytical method is very time consuming. Fig. 6a and 6c represents the recovered coefficients and 6b as well as 6d illustrate the empirical errors of the two methods, i.e. analytical and Gaussian quadrature method, respectively. Empirical error plots show that even under the same conditions the empirical errors are less in the Gaussian quadrature method method.

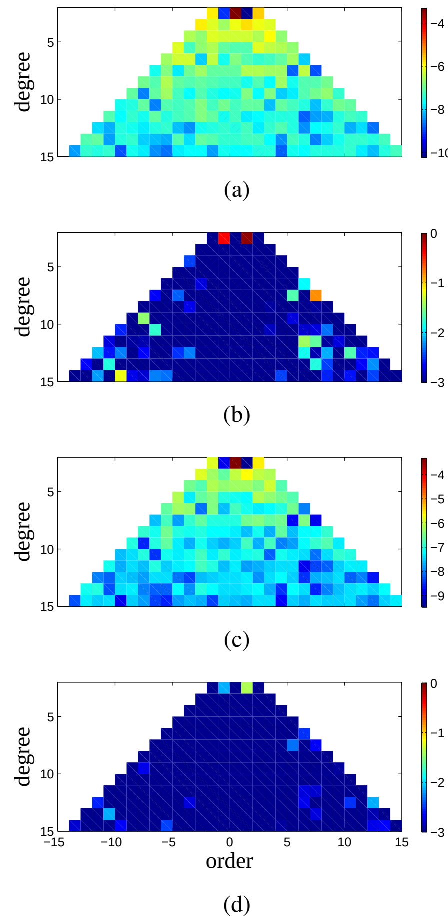

Fig. 6: Estimated SH coefficients and empirical errors recovered by analytical method(a-b), Gaussian quadrature method (c-d).

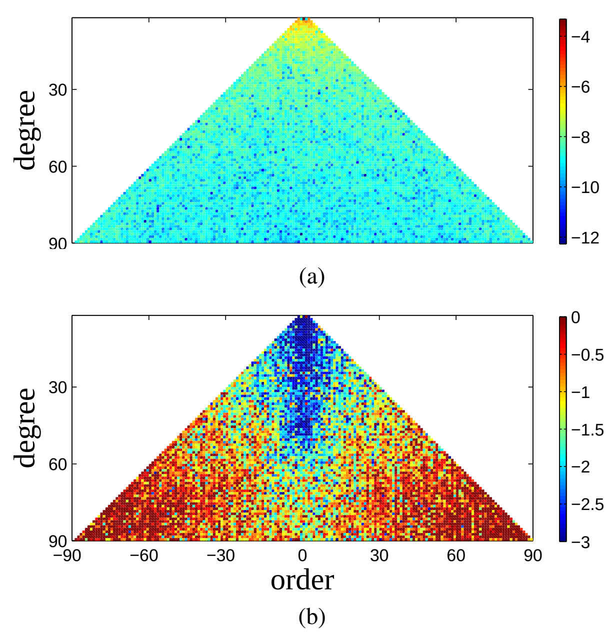

Fig. 7: Estimated SH coefficients and empirical error up to degree and order 90.

VII. Conclusion

The study concludes that the gravity recovery using the variational equation technique works faster when implemented using the variation of constant method. Here, in the Fig. 7 the SH coefficients up to the degree and order 90 are presented along with the empirical error plot. It took almost four hours to recover these results with a computer containing a 3.4 GHz processor. Please note that the algorithm is written in Matlab and it is expected that the efficiency of the algorithm would increase if it is programmed in C or FORTRAN. Fig. 5 illustrates the time consumption of the two methods. It display that, time requirement increases with the increase of SH coefficients. We can see that it is practically impossible to recover the same amount of SH coefficients using the direct method even if the simulation is run for several days.

References

Beutler, Gerhard (2005), *Methods of Celestial Mechanics: Volume I: Physical, Mathematical, and Numerical Principles*, chapter Variational Equations, 175–207. Springer Berlin Heidelberg, Berlin, Heidelberg.

Heiskanen, Weikko A. and Helmut Moritz (1967), *Physical Geodesy*. W. H. freeman and Co.

Jäggi, A., G. Beutler, and L. Mervart (2010), "Grace gravity field determination using the celestial mechanics approach first results." In *Gravity, Geoid and Earth Observation* (Stelios P. Mertikas, ed.), volume 135 of *International Association of Geodesy Symposia*, 177–184, Springer Berlin Heidelberg.

Keller, W. (2014), "Satellite-to-satellite tracking (lowlow/highlow sst)." *Handbook of Geomathematics*.

NASA, Press-Kit (2002), "Grace launch." *National Aeronautics and Space Administration*.

Rummel, R., G. Balmino, J. Johannessen, P. Visser, and P. Woodworth (2002), "Dedicated gravity field missions - principles and aims." *Journal of Geodynamics*, 33, 3–20.

Seeber, Günter (2003), *Satellite Geodesy*. Walter de Gruyter Berlin, New York.

Wermuth, Martin K. (2008), *Gravity Field Analysis from the Satellite Missions CHAMP and GOCE*. Ph.D. thesis, Technischen Universität München.